1.5 MW RF Load for ITER

Phase I Final Report

Calabazas Creek Research, Inc.
690 Port Drive
San Mateo, CA 94404
(650) 312-9575, Fax: (650) 312-9536
RLI@calcreek.com

Topic 23

Subtopic b

Principal Investigator: Dr. R. Lawrence Ives

This document contains no proprietary information.

Contents

Identification and Significance of the Problem or Opportunity, and Technical Approach

Calabazas Creek Research, Inc. (CCR) is developing 1.5 MW CW, RF loads for integration with the ITER reactor in France. These loads would also be used by gyrotron manufacturers and other fusion research facilities around the world. The RF load builds on more than fifteen years' experience with the 1 MW load developed under an SBIR program funded in 1996 (Figure 1) [1] . Several of these loads have operated for more than twelve years, and the experience gained provided the knowledge to develop 2.0 MW loads in a second DOE SBIR grant funded in 2009 [2]. Two 2.0 MW loads were delivered to JAEA in Japan, and one operated successfully at 1.62 MW [3]; which is the maximum power available from a long pulse gyrotron.

Figure 1. 1.2 MW RF load

Each of these loads utilized innovative schemes to dynamically sweep the incoming RF power around the load interior. RF loss material absorbs the power and conducts it to a high flow coolant system. The dynamic sweeping of the RF power avoids issues with constructive interference inside the load. Since the load is, by necessity, overmoded, the RF power reflects many times before it is totally absorbed. It is inevitable that constructive interferences will occur. If the constructive interference is near an interior surface, the very high RF loading will likely damage the load or generate localized gassing and arcing. No one has reported an RF load that matches the performance of the 1 MW loads developed by CCR in the 1990s. CCR's technological advantage was significantly increased with development of the 2 MW loads in 2010.

The 1 MW and 2 MW loads primarily used anodized aluminum structures. CCR developed a stainless steel and copper prototype under a UT-Battelle subcontract [4] that was designed to provide the same performance as the aluminum version; however, it has not yet been fully tested. Figure 2 shows a photograph of that load.

These loads use rotating structures to sweep the RF power around the load interior. The 1 MW load uses a shaft to rotate a reflector at the downstream end of the load. Designed for Gaussian mode input, the incoming beam impacts the reflector mirror and reflects toward the interior cylindrical load surface. The user must insure that the incoming RF beam impacts the downstream mirror with a specified profile. If the beam at the mirror is too large, RF power will impact static surfaces behind the reflector. If the beam is too small, the power density of

the reflected beam may damage the load surface. Since the mirror reflects RF power toward the input end of the load, approximately 5% of the RF power is coupled back into the waveguide. Most users install a preload to absorb this power. Figure 3 shows a Toshiba preload attached to a CCR load at JAEA.

Figure 2. 2 MW CW RF load

CCR initially installed u-shaped, plastic seals around the rotating shaft to maintain load vacuum and seal the coolant channels. These worked well for hundreds of operating hours, but were difficult to maintain. The design was upgraded to ferromagnetic seals around 2005, and loads with these seals required no subsequent maintenance. 1 MW loads are currently operating in Germany, Korea, Japan, and the U.S.

As gyrotron power increased, it became necessary to develop a load capable of dissipating more than 1 MW; consequently, CCR developed a 2 MW CW RF load in 2010. A record 1.5 MW of RF power was demonstrated at JAEA using one of these loads [5]. Subsequent tests increased the dissipated load power to 1.6 MW for 1.2 seconds and 1.38 MW for 5 seconds [3].

Instead of a rotating reflector at the downstream end of the load, the 2 MW loads use a rotating, corrugated waveguide and mirror launcher at the input. The RF input power is transmitted in an HE_{11} mode, and the waveguide-launcher configuration provides precise control of the RF. Not only does this provide control of the heat density profile, but the configuration avoids coupling RF power back into the input waveguide. Measurements indicated less than 1% of the RF power escapes the load, eliminating requirements for a preload. Two ferromagnetic seals maintain vacuum around the rotating waveguide-launcher.

Figure 3. JAEA load with preload

The ITER facility will require twenty eight loads capable of dissipating 1.4 MW of long pulse RF power [5]. Since this is a nuclear facility, stringent specifications apply to all devices in contact with vacuum or cooling systems. The specifications include [6]:

- No materials subject to corrosion are allowed in coolant systems,
- No braze alloys are allowed between coolant and vacuum,
- No demountable seals between water and vacuum,
- Non-metal vacuum seals are not allowed,
- Ferrofluids are not allowed for vacuum seals.

These specifications eliminated CCR's 1 MW and 2.0 MW loads from consideration for ITER. Consequently, the Phase I program initiated development of a 1.5 MW CW, RF load that uses no rotating structures through the vacuum envelope, eliminating rotating seals. The new design also eliminates non-metal vacuum seals and incorporates an innovative bellows

configuration with a pivoting joint to support the reflector. The bellows allows a revolving reflector to sweep the RF power without a rotating shaft through the vacuum envelope. The shaft is welded to the bellows, and the bellows assembly is mounted to the load using metal seals.

Figure 4 shows the new reflector assembly where the reflector orbits around the input waveguide. The assembly in Figure 4 incorporates a dummy fixture on the shaft to duplicate the weight of the reflector filled with coolant. This configuration allowed realistic testing of the assembly in the most stressful orientation during the Phase I program.

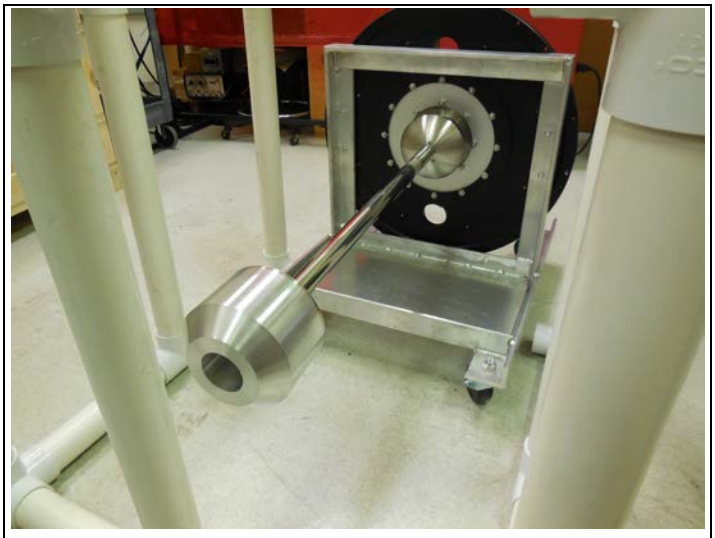

Figure 4. Orbiting reflector assembly in test fixture

The Phase I program generated a load design that eliminates ferrofluids, braze joints in the vacuum envelope, and O-ring seals between coolant fluids and vacuum. Details of the designs are described below.

In addition to the load, suppliers must also provide a control system to display diagnostic information, determine peak and average power, energize load systems, and provide appropriate interlock signals in case of a fault. CCR developed similar systems for the 1 MW and 2 MW loads. The Phase I program used this experience to develop a new system based on programmable logic controllers (PLC) with increased functionality and lower cost.

In summary, the Phase I program developed a preliminary design of a 1.5 MW CW RF load meeting the current ITER specifications. During the Phase II program, CCR will complete the design and build a prototype RF load and electronic control system. This will be tested with the highest power RF source available to confirm the performance of the load and control system.

Anticipated Public Benefits

If successful, this program will develop a 1.5 MW RF load for ITER. The U.S. is responsible for providing twenty eight loads during the initial phase of ITER, with twenty four additional loads for a future upgrade. Currently, there are no RF loads that can meet the required specifications. This load will allow the U.S. to meet its ITER commitment as well as provide an advanced load for gyrotron developers around the world. It will maintain the U.S. as the leading supplier of RF loads capable of dissipating more than 1 MW CW of gyrotron power.

Degree to which Technical Feasibility has been Demonstrated

The Phase I Program

Technical Objectives

The objective of the Phase I program was to develop an RF load meeting the ITER specifications for testing high power gyrotrons in the electron cyclotron heating (ECH) system. A secondary objective was development of an electronic control system to measure gyrotron performance, monitor load operation, and provide interlock signals for system protection. These objectives were achieved through the following tasks:

1. Develop system for sweeping RF power without rotating seals for vacuum operation,
2. Optimize RF power distribution,
3. Develop assembly techniques to avoid braze alloys or non-metal seals between coolant and vacuum,
4. Design hardware and software for controlling load operation, monitoring gyrotron performance, and providing interlock signals for system protection.

The results of these tasks are described below:

Task 1 Develop system for sweeping RF power without rotating seals for vacuum operation

ITER specifications eliminate options for rotating components using ferromagnetic fluids or non-metal seals. Consequently, CCR developed a bellows-based, RF sweep system that provides the same functionality without ferrofluids or non-metal vacuum seals. The design uses a reflector mounted on a shaft that is revolved around the input waveguide, as illustrated in Figure 5. The reflector does not rotate, but is swept around the input waveguide to reflect RF power to the load cylinder. The motor revolves the reflector at approximately 26 revolutions per minute (RPM), identical to CCR's previous loads. The vacuum seal is provided by a bellows at the downstream end. The angular deviation of the shaft from purely axial is approximately 5^o, so the bellows should exhibit unlimited lifetime. The shaft provides water cooling to the reflector and support shaft. An advantage of this design over previous configurations is that the shaft will provide additional reflection of RF power, further reducing loading following the initial impact.

Figure 6 shows the interior configuration of the support structure for the revolved reflector. The vacuum seal is provided by the bellows, which is welded to the support shaft and a flange that mates to the load endplate. The air-side end of the shaft is mounted in a pivot bearing and revolved by a motor using a chain drive. The motor is the same type used in all CCR loads. CCR loads have used these motors since 1999 without a single failure.

The primary concern was robustness of the support assembly to horizontal operation. This places the maximum stress on the bearings and support structures. During the Phase I program, the assembly shown in Figure 6 was built and tested. Figure 7 shows the assembly

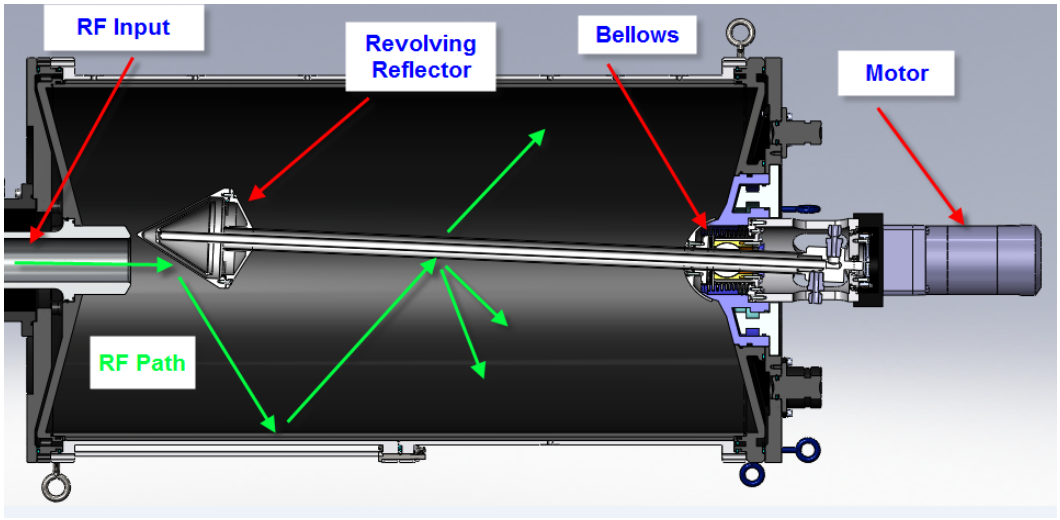

Figure 5. Sliced view of revolved reflector load

mounted in a test structure for horizontal operation. The reflector was replaced by a dummy structure that provided the same weight as the final reflector filled with coolant.

The assembly was operated for more than 400,000 cycles over 315 hours. A video of the rotating assembly is available at www.calcreek.com/1-5-mw-rf-load-reflector-testing/. The testing exceeded expectations, and the assembly was operating well when testing was terminated. The structure was disassembled and the components examined for excessive wear. Minor changes improved the pivot bearing, though it was still functional when testing was terminated. All vacuum components were intact and performing as designed.

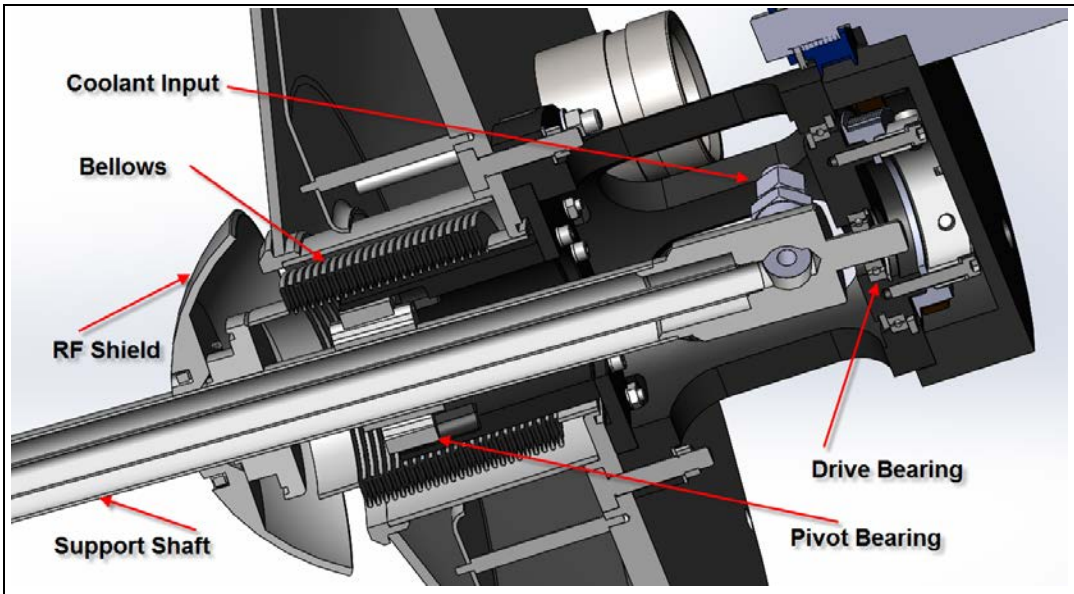

Figure 6. Solid model of revolving reflector support assembly

The Phase I program validated the design of the revolving reflector assembly, even for the most stressful orientation. Only minor modifications are anticipated to improve the design. Development of this assembly in complete, an it is not anticipated that further modifications will be required before implementation into deliverable loads.

Task 2. Optimized RF power distribution

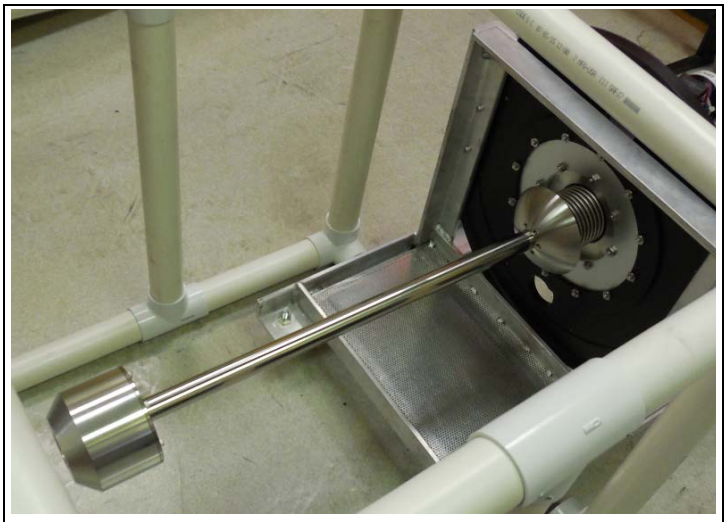

Figure 7. Test revolving reflector assembly in test structure

Several factors were analyzed to develop the power distribution design. As illustrated in Figure 8, input power enters the load through a corrugated, HE_{11} waveguide and impacts the conical surface of the revolving reflector, which deflects the power to the cylindrical wall of the load. The reflector must reflect the full, 1.5 MW of input power without damage. Analysis is complicated by the revolving operation of the reflector. As the reflector is swept around the input port, the region of RF impact revolves around the reflector cone. This significantly reduces the average power imposed on any region of the reflector but introduces cyclic fatigue issues.

The shape of the cone determines the distribution of the power on the cylindrical wall. The goal is to minimize the peak power density at the wall by optimizing the axial shape of the mirror. Consequently, the final design of the reflector surface was curved to maximize axial power distribution. Figure 9 shows the profile developed during the Phase I program.

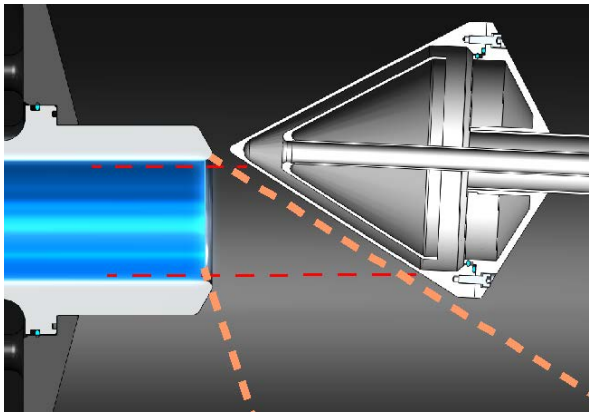

Figure 8. Orientation of revolving reflector and input waveguide showing path of RF power

SURF3D was the principal RF code used during the optimization process. SURF3D, developed in previous SBIR programs, uses surface field integral analysis to predict the electromagnetic field patterns launched from a metal surface [7,8]. SURF3D was a revolutionary code that dramatically improved performance of quasi-optical launchers in gyrotrons. It was instrumental in design of CCR's 2 MW CW load.

SURF3D inputs the HE_{11} field pattern from the input waveguide and models the reflection from the reflector surface. The code calculates the radiation through space and determines the

power density distribution on the cylindrical wall. Figure 10 shows the power density incident on the cylinder wall for 1.5 MW of input power using the conical surface shown in Figure 9.

The next analysis determined the thermal stresses imposed on the stainless steel inner load cylinder. Previous loads used aluminum or copper cylinders, which provide much higher thermal conductance. There was concern that the reduced conductivity of stainless steel, coupled with the higher RF intensity compared to previous loads, would incur higher thermal stresses. This was confirmed by the analysis, which also demonstrated that the stresses were significantly below the working strength of the material.

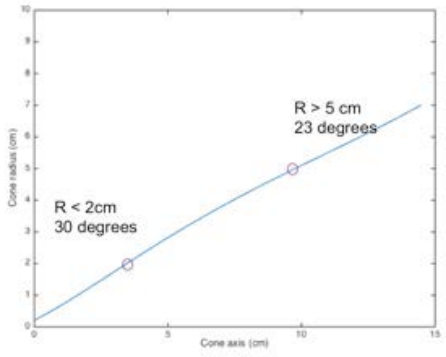

Figure 9. Profile of conical reflector

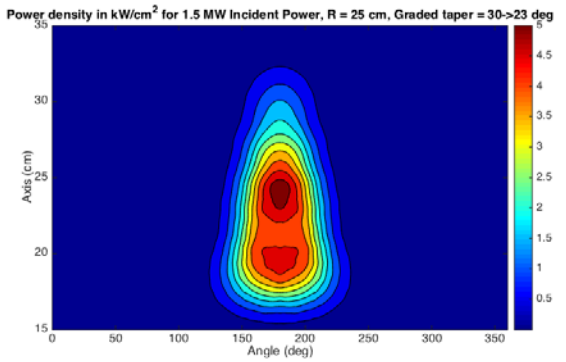

Figure 10. RF power density on cylindrical wall for 1.5M MW input power

The analysis simulated the cyclical heating of the cylinder imposed by the rotating reflector. Figure 11 shows the trapezoidal power profile imposed on the wall section shown in Figure 12. The wall material was 304L stainless steel with an initial temperature of 25C. Convection cooling was imposed on the fins appropriate for 250 GPM of water flow with an ambient temperature of 40C. The peak absorbed power density for the pulses shown in Figure 11 was 3.5 kW/cm^2. The analysis assumed 0.7% of the RF power was absorbed by the stainless steel with the balance reflected, consistent with the conductivity of the material [10]. The power ramps up to full power in 0.1 seconds, remains at the peak for 0.1 seconds, then ramps down

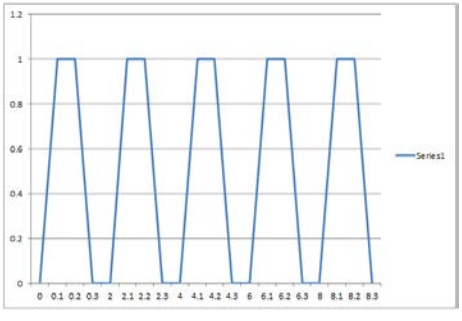

Figure 11. Imposed power density profile. The RF power is cycled every two seconds.

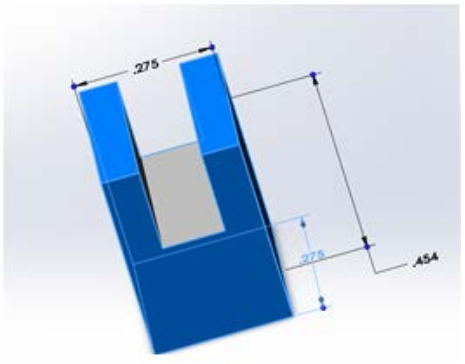

Figure 12. Cylindrical wall section used in thermomechanical analysis. Dimensions are in inches.

over 0.1 seconds. This cycle repeats every two seconds.

Figure 13 shows the peak temperature on the inner wall through 600 seconds of operation. The performance stabilizes after 25 seconds with the maximum temperature just below 52C. The minimum temperature between pulses is approximately 44C. Figure 14 plots the peak stresses through 50 seconds of operation. The peak stress is less than 95 MPa, well below the yield stress of 262 MPa. This indicates that loss material can be applied in this region without exceeding the yield stress of the stainless steel.

The analysis was repeated and the absorbed power increased until the inner wall temperature reached approximately 350C. This temperature was achieved assuming 20% absorption of the incident RF power. This corresponds to a loss coating thickness of 0.005 inches, which is slightly less than in the copper and aluminum loads (0.006 inches). The peak stresses, however, approximately equal the yield stress. Consequently, CCR will apply a loss coating that absorbs approximately 10% of the incident power, ensuring that the peak stresses are well below levels of concern.

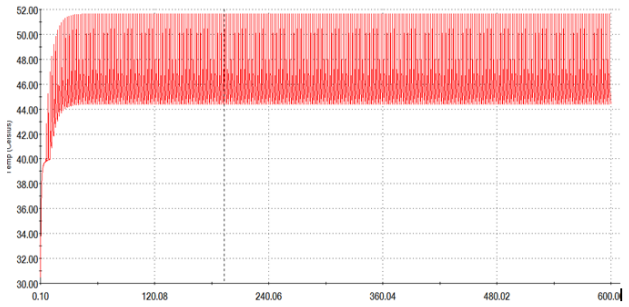

Figure 13. Maximum temperature on inner wall through 600 seconds of operation

The RF power reflected by the wall will directly impact the support shaft for the revolving reflector. This power will be both azimuthally and axially scattered around the load, eliminating any additional thermal hot spots. The loss coating in these regions will be increased to absorb approximately 70% of the incident power. The support shaft is heavily cooled, so heating is not an issue.

The program analyzed the performance of the reflector cone, which must reflect up to 1.5 MW CW of RF power without incurring excessive thermal stresses. Figure 15 shows the SURF3D calculation of the incident power density, which exceeds 70 kW/cm^2. As the reflector revolves around the load input, the incident RF power revolves around the cone. Therefore, examination of the performance requires a transient analysis.

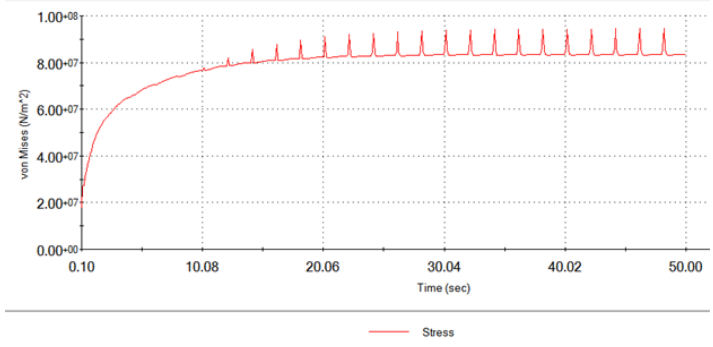

Figure 14. Peak stresses through 50 seconds of operation

The initial analysis assumed a stainless steel reflector; however, the simulation determined that the water cooled surface would oscillate between 109C and 199C, which is clearly excessive. Simulations assuming a copper coating on a stainless steel reflector provided

significantly better performance, as shown in Figure 16 and Figure 17 showing the vacuum wall and wet wall temperatures, respectively. The maximum stress is approximately half the yield strength of the material.

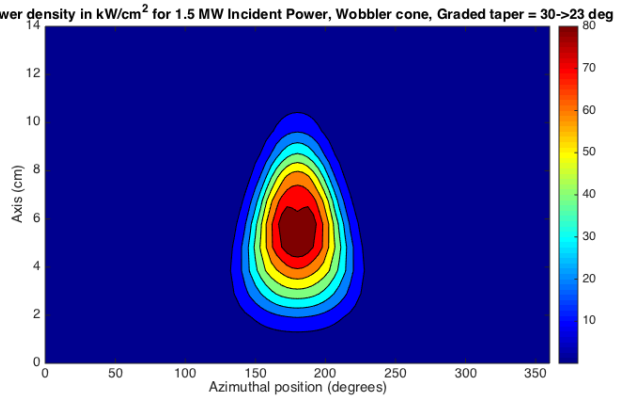

Figure 15. Incident RF power on reflector cone

CCR investigated plasma spraying a copper coating onto the stainless steel cone. Plasma spraying is a standard process used in manufacturing turbine blades in jet engines. According to CCR's plasma spray vendor, a reliable copper coating can be applied with a thickness up to 0.010 inches (0.254 mm), which is significantly greater than the skin depth (approximately 0.160 microns) [11]. The plasma spraying process uses temperatures significantly higher than the surface will see in operation. Consequently, plasma spraying should provide a robust coating for this application.

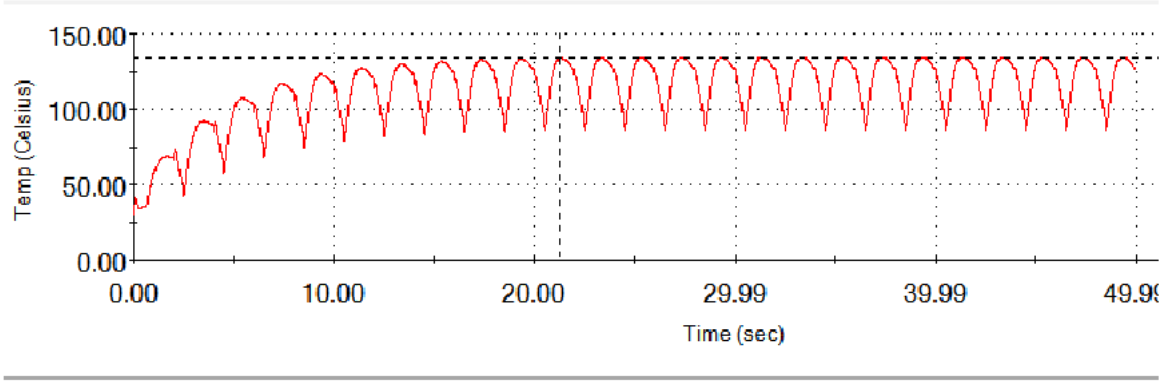

Figure 16. Vacuum wall temperature for copper coated stainless steel reflector

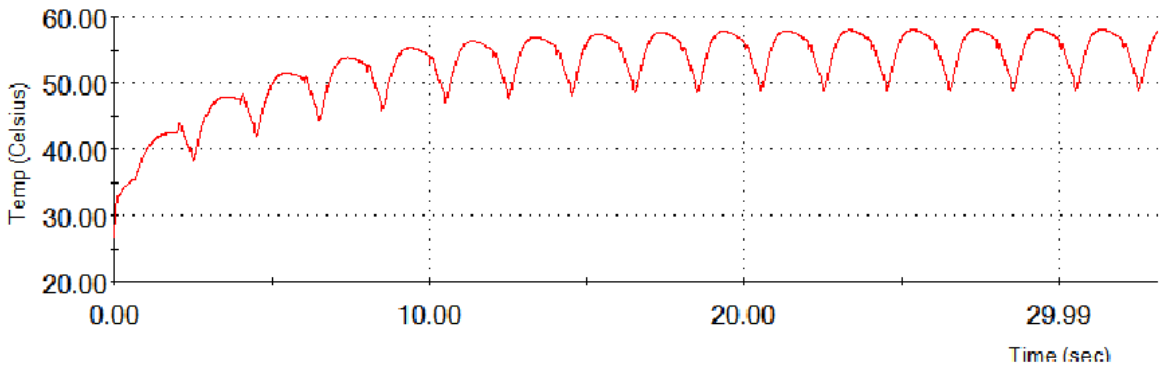

Figure 17. Wet wall temperature for copper coated stainless steel cone

The analysis and performance of the 2 MW CW RF load clearly indicates that an all copper reflector can safely handle more than 1.5 MW. To build an all copper cone assembly, however, it will be necessary to bond the copper to a stainless steel weld flange so the assembly can be welded to the support shaft. Since braze alloys are not allowed in water to vacuum joints, this bond would be obtained using explosive bonding.

This task demonstrated that designs are available to handle the power deposition on the reflector and the primary loss surfaces in the load. Remaining tasks include finalizing the reflector design and generating the drawings.

Task 3. Develop assembly techniques to avoid braze alloys and non-metal seals

The program initially considered a number of bonding techniques to avoid brazing, including electron beam welding and explosive bonding. It was determined that the most cost effective approach was to fabricate the load cylinder and end plates from stainless steel and bond components, where appropriate, using tungsten inert gas (TIG) welding. Since the ITER specifications prohibit demountable joints between water and vacuum, the end plates will be welded to the inner load cylinder. The input waveguide assembly and the reflector support assembly will be mounted to the end plates using all metal Helicoflex seals.

End plates for the 2 MW load delivered to DOE-ITER used welded and machined stainless steel end plates. Figure 18 shows one of these endplates with a copper, vacuum pumpout port. This end plate was tested to 200 psi, significantly higher than the 150 psi required for ITER.

Figure 18. Stainless steel end plate for DOE-ITER load, including copper sieve vacuum port

The Phase I load design uses one stainless steel cylinder to provide the loss surfaces with a second, outer cylinder forming the cooling channels. The inner cylinder provides the loss coating on the inner diameter and longitudinal fins on the outer diameter for heat transfer to the water coolant. The outer cylinder is bolted to the end plate cover assemblies. ITER specifications do not prohibit non-metal seals between water and air, so the current design uses O-rings to seal the outer cylinder to the end plates. These can be converted to Helicoflex seals if the specifications change.

Several methods are available for fabricating the stainless steel cylinders. A common practice is to roll metal plate into a cylinder and weld the interface. This is an economical approach; however, it results in significant stresses in the material. This leads to warpage when axial

grooves are machined on the outer diameter, and it becomes very difficult to maintain the tolerance on the wall thickness in the grooves and the interface features at the ends. It also complicates assembly of the inner and outer cylinders. Forgings can be expensive, and castings are discouraged for use in ITER devices as they are subject to porosity and inclusion issues.

Centrifugal spinning provides and attractive alternative. In this approach, molten metal is poured into a cylindrical form which is rapidly spun to force the metal into a cylindrical shape. When the metal is cooled, it contains negligible residual stresses. Consequently, the cylinder maintains its shape as the axial grooves are machined. CCR implemented this approach for the 2 MW loads shipped to JAEA with excellent results. Figure 19 shows the spin casting of an inner cylinder. Additional effort, however, is warranted to fully evaluate the cost effectiveness of various fabrication approaches. In the Phase II program, CCR will further investigate cylinder fabrication techniques to arrive at the most cost effective approach.

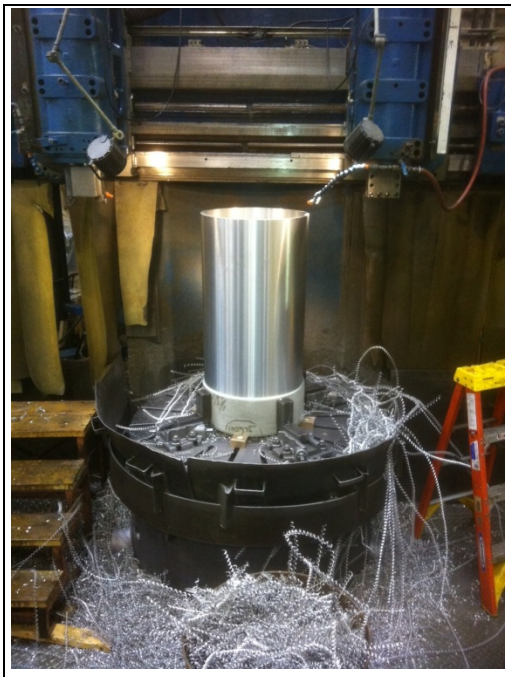

Figure 19. Centrifugally spun aluminum cylinder following rough machining of the outer diameter

Task 4. Control hardware and software

The control system provides a single point of operation for all interlocks and sensors for the load and determines the dissipated RF power. The system consists of two modules. The main controller resides in the user control area and provides information to the operator, including load operation and interlock signals. The Remote Sensor Unit collects data from the sensors, including resistive temperature devices (RTDs), proximity sensor, and flow sensors, and formats and transfers the information to the control console.

The controller system includes the following features:

- On/Off control for the revolving reflector motor,
- Measurement of the reflector revolution rate,
- Measurement of the reflector assembly coolant flow rate,
- Measurement of the main load coolant flow rate,
- Monitoring of inlet and outlet coolant temperatures,
- Determination of average RF power for short pulse or CW operation,
- Determination of peak RF power for short pulse or long pulse operation,
- Interlock for main coolant flow,
- Interlock for reflector revolution,
- Interlock for reflector coolant flow,

- Interlock for arc detectors,
- Digital output of signals for remote processing or control.

The system includes the following components

- Rack mounted, central control console with diagnostic monitoring and load interlocks,
- Remote module for signal conditioning and transmission to the control console,
- Digital cable connecting the remote module to the control console,
- Flow meter for monitoring reflector coolant flow,
- High flow turbine for main coolant flow monitoring,
- Resistance Temperature Devices (RTDs) for measuring input and output coolant temperatures,
- Proximity detector for monitoring reflector revolution,
- Auxiliary plumbing for the coolant systems.

The original system was designed in the late 1990s, and the software was upgraded in 2012. The Phase I program completely redesigned the hardware using programmable logic controllers (PLCs) and signal conditioning modules. This eliminates custom printed circuit board fabrication and much of the manual assembly required for the previous controller, providing increased functionality and lower cost.

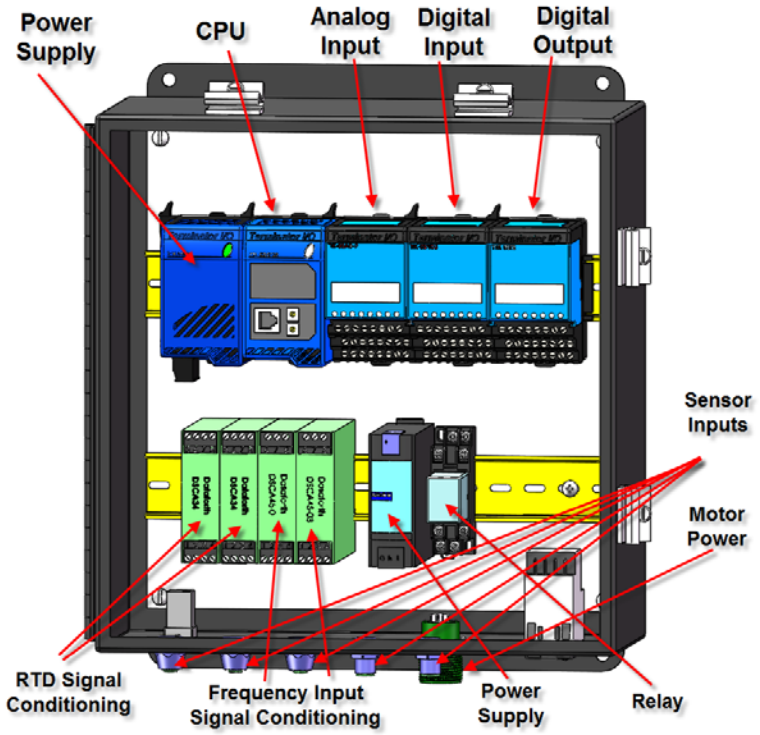

Figure 20. Solid model of internal layout for Remote Sensor unit with front panel removed

Figure 23 in the Appendix shows the circuit schematic for the Remote Sensor Unit, and Figure 20 shows a solid model of the associated hardware. This unit collects sensor data from the RTDs measuring the inlet and outlet coolant temperatures, the flow rates for the main coolant flow and reflector flow, and the rotation sensor for the reflector. These signals are transmitted to the signal conditioning modules shown in Figure 18 (green blocks), which isolate the downstream electronics from electrical noise and transmit the signals to analog-to-digital converters connected to the CPU module. The power supply for the reflector motor is

controlled by the CPU through a relay on the lower rail. Data collected in the Remote Sensor Unit is transmitted to the control console through a shielded CAT6 ethernet cable. This unit is located near the load to minimize the length of sensor cables.

Figure 24 in the Appendix shows the schematic for the main control console, Figure 21 shows the main controller with a 15-inch Touch-Screen display, and Figure 22 shows the interior layout. The main control unit resides in the user control room and allows operation of the load and display of the sensor readings and calculations of peak and average power. The system can also be configured to transmit operational and diagnostic information to a remote control and data storage system.

It also provides interlocks to terminate gyrotron operation if a load fault is detected. Load faults can be cause by electrical arcs, insufficient coolant flow, or non-revolution of the reflection mirror. The PLC system provides status, testing, and reset of all interlocks. The interlock for critical faults, such as the arc detector, transmits signals directly to the primary control system to rapidly shutdown the gyrotron power supply or RF power generation to prevent damage to the load or ECH system.

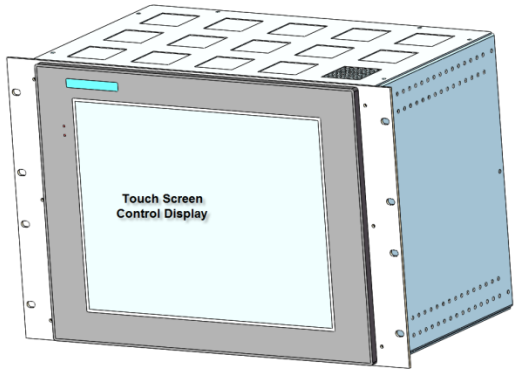

Figure 21. Main controller

PLC's allow low cost assembly with the ability to update and modify operation through the CPU module software. The modules also allow simple maintenance and troubleshooting in the event of a component failure.

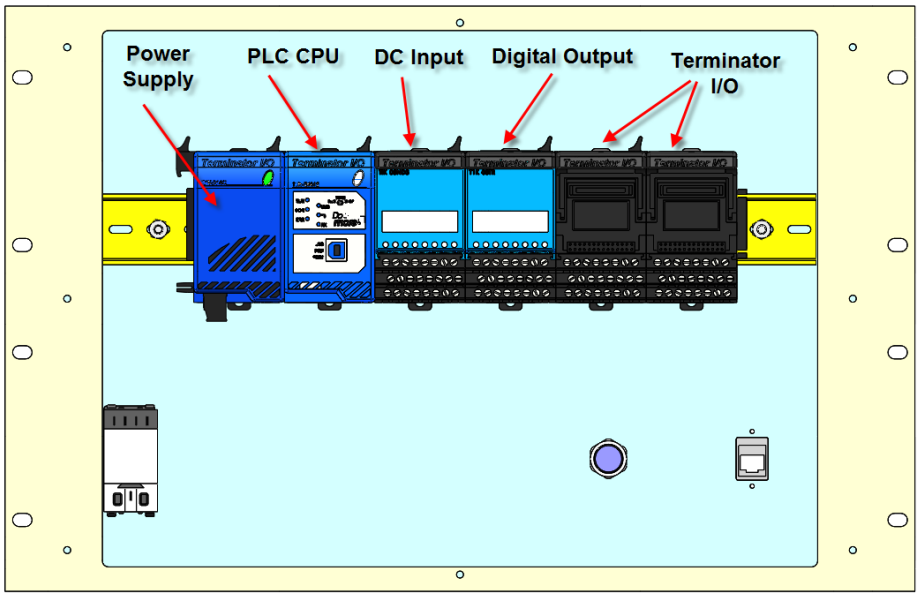

Figure 22. Interior layout model of main control unit

The next step in developing the control system is to build and test the prototype design. This is scheduled for early in the Phase II program.

Supplemental Task

Though not planned for the Phase I program, CCR investigated options to reduce reflection of RF power from the load back into the transmission line. ITER specifications limit reflected power to less than 0.25% in the HE_{11} mode and less than 0.5% total. A technique was reported by Sobolev et al to reduce transmission of non-HE_{11} modes using waveguide gaps [12]. This provides a technique to prevent back propagation of reflected RF power and allows implementation of a waveguide gap for vacuum pumping. Sobolev provides formulations for optimizing the gap to minimize losses in the primary load while diffracting higher order modes out of the transmission line. The Phase II program will investigate these and other formulations to design a filter to minimize reflected power and enable vacuum pumping of the load.

Summary

The Phase I program successfully updated the design of CCR loads to meet the current ITER specifications. Rotating ferromagnetic and non-metal vacuum seals were eliminate, as were all brazed vacuum joints, and the design does not use corrosive materials in the coolant system. Detailed thermal analysis indicates the new design can safely absorb the incoming RF power without exceeding allowable material stresses. The electronic control system was redesigned to incorporate the latest technology for system monitoring and control. Analysis indicates the load can provide the same, highly reliable performance as CCR's previous loads.

In the Phase II program, CCR will complete the development and build and test a prototype load. This will require finalizing the design of the reflector cone, finalizing the vacuum pumpout/reflection suppression system, completing the mechanical design of the endplate assemblies, and generating the complete drawing package.

References

1. Development of a High Power CW Waterload for Gaussian Mode Gyrotrons, U.S. DOE Grant No. DE-FG03-95ER81938, August 1995 through August 1998.
2. Development of a 2 MW CW Waterload for Electron Cyclotron Heating Systems, U.S. DOE Grant No. DE-DC0001930, July 2009 through August 2012.
3. Takayuki Kobayashi, Japanese Atomic Energy Agency, private communication, March 2016. Results to be published at IAEA fusion energy conference, Kyoto, Japan, in October 2016.
4. UT-Battelle, LLC Subcontract No. 4000105183, May 2011.
5. T. Kobayashi et al. "Progress and Status of the Gyrotron Development For The JT-60AS ECH/CD System," IEEE IRMMW-THz Conference, Hong Kong, August 2015.

6. G. Hanson et al, “ITER ECH Transmission Line Overview,” ECH Technical Community Meeting, Oak Ridge National Laboratory, May 2014.
7. U.S. ITER Technical Specification ECH Prototype Dummy Load, US ITER 1050101-PD0014-R00.
8. “Optimal Synthesis of QO-Launchers,” U.S. DOE Grant No. DE-FG03-00ER82965, June 2000 through August 2004.
9. “Advanced Quasioptical Launcher System,” U.S. DOE Grant No. DE-FG02-05ER84181, Au-gust 2006 through February 2010.
10. http://explosionbonding.com/
11. W. Kasparek, A. Fernandez, F. Hollmann, R. Wacker, “ Measurements of Ohmic Losses of Metallic Reflectors at 140 GHz Using a 3-Mirror Resonator Technique,” Intern. Jou. of Infrared and Millimeter Waves, Vol. 22, No. 11 November 2001.
12. Derek Needam, Plasma Coating Corporation, private communication, March 1, 2016.
13. D.I. Sobolev et al, “Minimization of Diffraction Losses in Big Gaps in Multi-Mode Waveguides,” Intern. Jou. Infrared and Millimeter Waves, Vol. 26, No. 7, July 2005.

Appendix

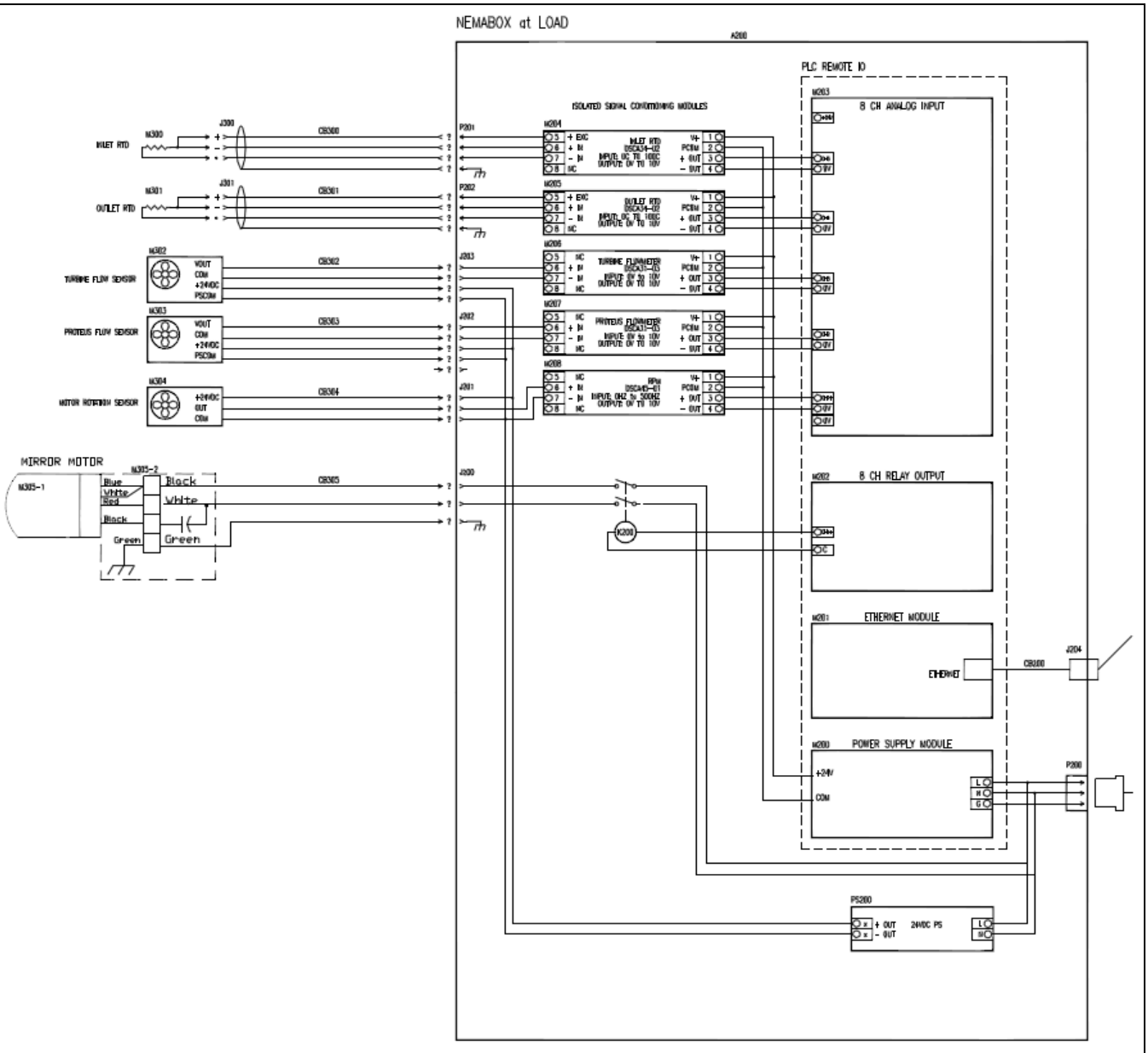

Figure 23. Circuit schematic for remote sensor controller

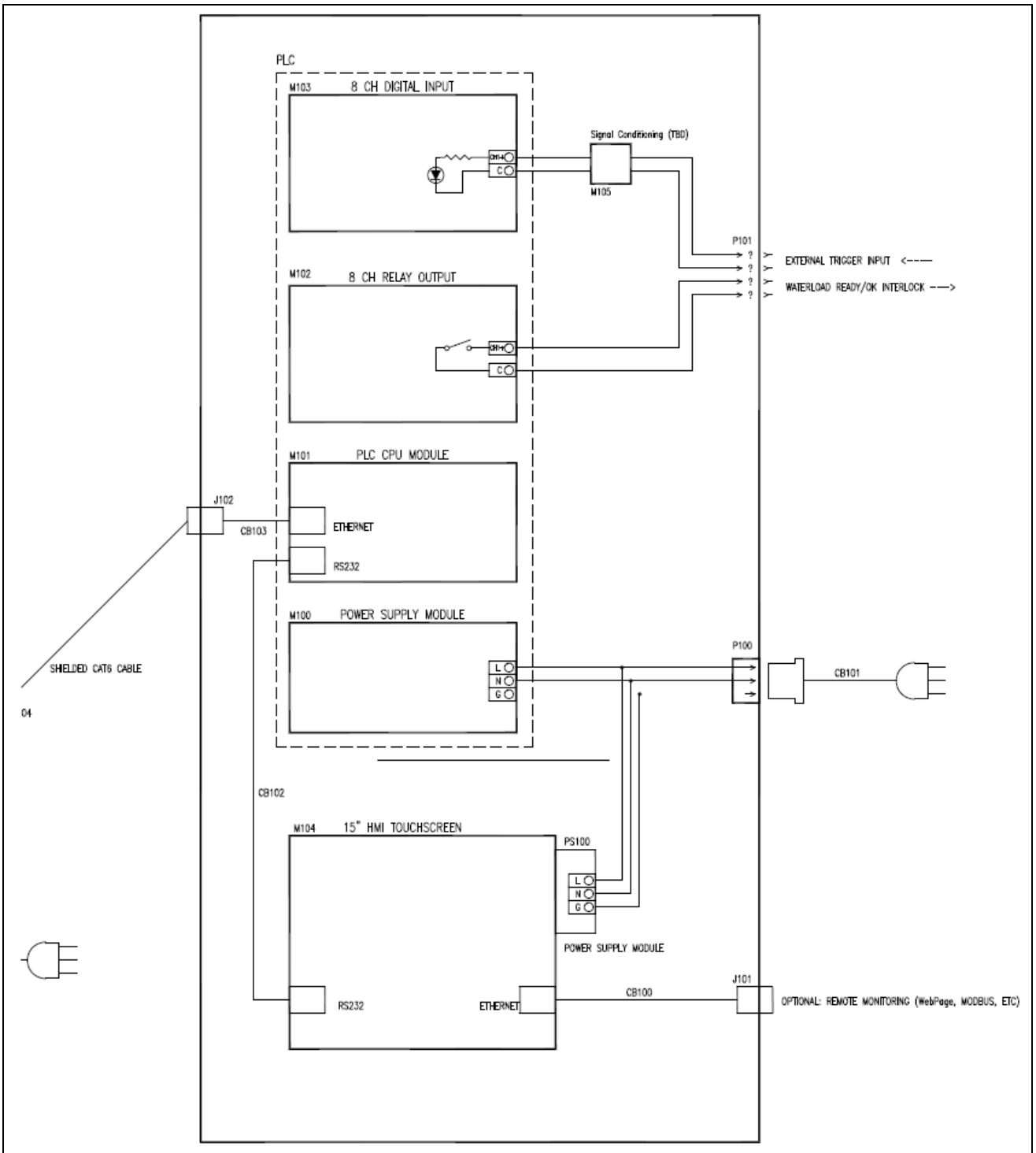

Figure 24. Main control console schematic